RSC Advances

PAPER

View Article Online
View Journal | View Issue

Cite this: *RSC Adv.*, 2018, **8**, 9211

Mechanisms of partial hydrogen sorption reversibility in a $3NaBH_4/ScF_3$ composite

Ning Zhao,[a] Jianxin Zou, *[ab] Xiaoqin Zeng[ab] and Wenjiang Ding[ab]

Received 15th January 2018
Accepted 23rd February 2018

DOI: 10.1039/c8ra00429c

rsc.li/rsc-advances

A new hydrogen storage composite containing $NaBH_4$ and a 3d transition metal fluoride, $3NaBH_4/ScF_3$, was synthesized *via* ball milling. The composite shows no reaction during milling and its dehydriding process can be divided into three steps upon heating: (i) partial substitution of H^- by F^- in $NaBH_4$ to form $NaBH_xF_{4-x}$ at the early stage, releasing about 0.19 wt% of hydrogen; (ii) formations of Na_3ScF_6, $NaBF_4$ and ScB_2 through the reaction between $NaBH_4$ and ScF_3, with 2.52 wt% of hydrogen release and a dehydriding activation energy of 162.67 kJ mol^{-1} H_2; (iii) further reaction of residual $NaBH_4$ and Na_3ScF_6 to form NaF, B and ScB_2, with a dehydriding activation energy of 169.37 kJ mol^{-1} H_2. The total hydrogen release of the composite reaches 5.54 wt% at 530 °C. The complete dehydrided composite cannot be rehydrogenated while the products after the second dehydriding step can be hydrogenated with an absorption activation energy of 44.58 kJ mol^{-1} H_2. These results demonstrate that by adding 3d transition metal fluorides into $NaBH_4$, a partial reversibility in $NaBH_4$ can be achieved.

1 Introduction

Hydrogen is one of the most promising alternative and attractive clean energy sources that can substitute fossil fuels, with sufficient energy density and environment-friendliness.[1,2] Nevertheless, almost a century since the concept of "hydrogen economy" was introduced by Jules Velne,[3,4] it is still challenging to find reliable, flexible and cost-efficient hydrogen media for on-board, stationary and portable applications.[5,6] In the past few decades, great attention has been paid to both hydrogen production technologies and a variety of hydrogen storage methods,[7–10] including the use of different compounds,[11,12] especially complex hydrides, of which borohydrides are typical representative.[13–15] These solid-state hydrogen storage materials offer some advantages over high pressure gaseous storage and low temperature liquid storage, such as high capacity, high safety, and low cost. In particular, alkali metal borohydrides are regarded as possible hydrogen carries, ascribed to their contribute to their high gravimetric and volumetric hydrogen density, together with good stability.[16] However, current research results showed that few technologies regarding the use of metal borohydrides as hydrogen storage carriers are able to fulfill the requirements established by the US Department of Energy.[17]

Early investigations into borohydrides have shown that, compared to other borohydrides such as $LiBH_4$ and KBH_4, $NaBH_4$ is stable under alkaline conditions, and undergoes hydrolysis through the following reaction:[18]

$$NaBH_4 + 4H_2O \rightarrow NaBO_2 \cdot 2H_2O + 4H_2 \quad (1)$$

However, the use of $NaBH_4$ as a hydrogen generator through hydrolysis faces several issues related to the catalyst durability, and/or poisoning, as well as storage vessels.[19–21] In contrast, thermal decomposition of $NaBH_4$ has emerged as potential alternative method for hydrogen storage. J. Urgnani *et al.* investigated the thermal decomposition behaviors of $NaBH_4$, and proposed that $NaBH_4$ would decompose in two steps according to the following reactions:[22]

$$NaBH_4 \rightarrow NaH + B + \frac{3}{2}H_2 \quad (2)$$

$$NaBH_4 \rightarrow Na + B + 2H_2 \quad (3)$$

For the sake of improving the thermodynamic and kinetic properties of the thermal decomposition of $NaBH_4$, many strategies have been taken, such as adding catalyst, building thermodynamic destabilization system, nano-engineering and chemical modifications.[13,23–25] For instance, $NaBH_4/MgH_2$ system could fulfil its decomposition before melting due to the formation of MgB_2 in the system.[26] Czujiko *et al.* suggested that pure Mg could lower down the desorption temperature of $NaBH_4$ through catalytic effect.[27] In addition, the decomposition of $NaBH_4$ may occur at lower temperatures with some reversibility through the addition of Ni-based catalysts,[28] which

[a]National Engineering Research Center of Light Alloy Net Forming, State Key Laboratory of Metal Matrix Composites, Shanghai Jiao Tong University, Shanghai, 200240, P. R. China. E-mail: zoujx@sjtu.edu.cn; Fax: +86-21-34203730; Tel: +86-21-54742381

[b]Shanghai Engineering Research Center of Mg Materials and Applications, School of Materials Science and Engineering, Shanghai Jiao Tong University, Shanghai, 200240, P. R. China

facilitates hydrogen release and improves the reversibility to some extent.[29] Moreover, the chemical reaction that regenerates borohydrides from metal–borides occurs much easier over the regeneration from boron since less energy is required for breaking the chemical bond between B–M (M means metal) relative to the B–B's.[30]

In previous works, many research works regarding hydrogen storage composite systems have been carried out, and some of them have explored how rare earth element (RE) addition can effect the thermodynamics and kinetics properties of metal borohydrides based systems, *i.e.*, $NaBH_4$–YF_3,[31] $NaBH_4$–$ScCl_3$,[32] $LiBH_4$–YCl_3,[33] *etc.* In particular, hydrogen sorption reversibility was achieved in $3NaBH_4/LnF_3$ systems with good thermodynamic and kinetic properties.[34]

Considering that scandium lies in the III B column of the periodic table as the lanthanide elements, we attempt to prepare a new hydrogen storage system, $3NaBH_4/ScF_3$, through ball milling method. Our previous investigations on $NaBH_4$–MF_3 (M = metal) systems proved that the molar ratio of 3 : 1 was the best one, *i.e.* $3NaBH_4/LnF_3$ (Ln = La, Ce, Nd, Gd, Yb),[34] $3NaBH_4/YF_3$,[31] $3NaBH_4/PrF_3$ and $3NaBH_4/HoF_3$.[35,36] If the molar ratio of $NaBH_4$ to MF_3 is higher than 3 : 1, some $NaBH_4$ will be left after the desorption due to the incomplete reaction. While if the ratio is less than 3 : 1, MF_3 is excessive, and the overall hydrogen sorption capacity is reduced since MF_3 can neither release nor absorb hydrogen. Consequently, the ratio of $NaBH_4$ to ScF_3 is set as 3 : 1 in the present work. We conducted a detailed study of hydrogen sorption behaviors of the $3NaBH_4/ScF_3$ system, and proposed mechanisms of hydrogen sorption in this composite, depending on experimental analyses.

2 Experimental

2.1 Sample preparation

$NaBH_4$ (Aladdin Reagent Database Inc., 96%) and ScF_3 (Aladdin Reagent Database Inc., 98%) were used as starting materials without further purification and mixed in the molar ratio of 3 : 1 in a planetary ball miller whose type is QM-1SP2. The stainless steel vessel with 100 ml volume was used to load 0.3928 g of $NaBH_4$ and 0.3530 g of ScF_3 powders together with 25 stainless steel balls (diameter of 5 mm, average weight of 0.8950 g each). The ball to powder weight ratio is approximately 30 : 1. Ball milling is conducted at a rotation speed of 400 rpm for 180 min. The prearrangement, manipulation and storage of specimen were carried out in an Ar-filled Lab 2000 glove box (Etelux inert gas system Co., Ltd.) in which neither moisture nor oxygen concentration beyonds 10 ppm.

2.2 Characterization

The analyses of phase composition for the ball milled, dehydrogenated and rehydrogenated samples were accomplished using an X-ray diffraction apparatus (D/max 2550VL/PC), equipped with a Cu-Kα radiation source. For XRD tests, composite powder at different states were kept into specific sample holders with arched glass on both sides and airtight PVC tape on the top, to isolate them from air. Meanwhile, the broad peak at around $2\theta = 15°$ in the patterns is caused by the tape. Using a Spectrum Nicolet iS5 produced by Thermo Fisher Scientific Inc., Fourier transform infrared spectroscopy (FTIR) tests were performed on samples with different states in an Ar filled glove box. In principle of volumetric methods, we carried out temperature-programmed-desorption (TPD) measurements on 0.2 g of the $3NaBH_4/ScF_3$ composite sample from room temperature to about 530 °C under an initial vacuum condition, with a heating rate R_H of 3 °C min^{-1}. Evaluations of hydrogen absorption performance were implemented for 10 h at various temperatures under around 3.2 MPa H_2 pressure.

Dehydrogenation behaviors of composites were determined by synchronous thermal analyzer (Differential Scanning Calorimetry/Thermal Gravimetry, DSC/TG), in a Netzsch, STA 449 F3 Jupiter equipment, in which R_H = 3 °C min^{-1}, 5 °C min^{-1}, 7 °C min^{-1} and 10 °C min^{-1}, respectively, starting from room temperature to about 500 °C, under the protection of 0.1 MPa Ar flow. To compare the properties of hydrogen storage performances of different composites, data of weight percent considering hydrogen release and uptake during the tests was assessed based on the samples' initial weight value.

3 Results and discussions

3.1 Dehydrogenation of the $3NaBH_4/ScF_3$ composite

The effect of the ScF_3 addition on the hydrogen desorption behaviors of $NaBH_4$ was examined by DSC measurements at different R_H, namely 3 °C min^{-1}, 5 °C min^{-1}, 7 °C min^{-1} and 10 °C min^{-1}, as well as TG measurement at the R_H of 10 °C min^{-1}, as Fig. 1 showed.

Two major endothermic peaks upon heating appeared on the DSC curves, indicating that two main desorption steps took place during dehydrogenation. According to the starting point of dehydriding in DSC profiles, the first major dehydrogenation begins at 356 °C with R_H = 3 °C min^{-1} heating rate condition. In contrast, pure $NaBH_4$ shows a dehydrogenation temperature of 517 °C under the same condition.[31] In addition, a subsequent broad endothermic peak was also recorded. TG curve obtained at the heating rate of 10 °C min^{-1} shows that the total mass loss reaches 4.10 wt% at 500 °C. According to the DSC/TG profiles, the dehydrogenation enthalpies of the first and second major desorption reactions are determined to be 27.43 ± 5 kJ mol^{-1} H_2 and 29.54 ± 2 kJ mol^{-1} H_2, respectively.

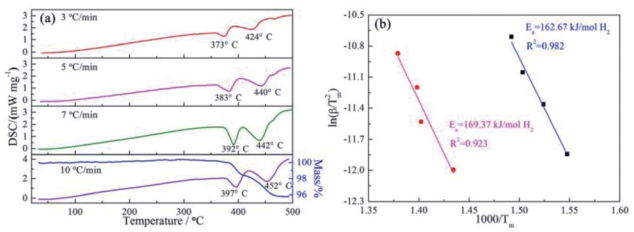

Fig. 1 DSC curves of $3NaBH_4/ScF_3$ composite samples under heating rates of 3 °C min^{-1}, 5 °C min^{-1}, 7 °C min^{-1} and 10 °C min^{-1} and TG profile at the heating rate of 10 °C min^{-1} (a) and the corresponding Kissinger plots for the two major endothermic desorption steps (b).

The apparent dehydrogenation activation energy (E_a) of the $3NaBH_4/ScF_3$ sample could be determined using the Kissinger method,[37] as described below:

$$\frac{d\left(\ln\frac{\beta}{T_m^2}\right)}{d\left(\frac{1}{T_m}\right)} = -\frac{E_a}{R} \quad (4)$$

where heating rate (β), peak temperature (T_m), and gas constant (R) show a specific relationship. Table 1 gives the peak temperatures in DSC curves at various R_H obtained from Fig. 1a. The fitting plot displays that $\ln(\beta/T_m^2)$ and $1/T_m$ have good linearity, as shown in Fig. 1b. According to eqn (4), the E_a value is calculated to be 162.67 kJ mol^{-1} H_2 and 169.37 kJ mol^{-1} H_2 for the first major desorption step and second major desorption step, respectively.

To obtain further information of dehydrogenation process of the target system, TPD measurement was performed on the ball-milled composite with a constant R_H of 3 °C min^{-1} from ambient temperature to 530 °C and the results are shown in Fig. 2. The results exhibit that $3NaBH_4/ScF_3$ composite has an appropriate onset dehydrogenation temperature, which is actually lower than 200 °C in vacuum. Meanwhile, the figure shows that the desorption behavior may be subdivided into three consecutive processes, with a small amount of hydrogen (~0.19 wt%) released at temperature lower than 310 °C in the initial process, and the latter two steps range from 310 °C to 420 °C, and above 420 °C, releasing about 2.52 wt% and 2.83 wt% of hydrogen, respectively. In comparison to the DSC measurements, the second and third desorption steps shown in TPD profile should correspond to the two major endothermic peaks on DSC curves.

The entire hydrogen release obtained from the experimental process up to 530 °C is 5.54 wt%, which is over 95% of the theoretical hydrogen content. Previous study shows that during dehydrogenation process of pure $NaBH_4$ under the same condition, only 0.68 wt% weight loss is observed when heated up to 482 °C.[19] Thus, the hydrogen desorption properties of $NaBH_4$ were significantly promoted by the addition of ScF_3. However, from Fig. 1, there is no endothermic peak present from ambient to 300 °C in DSC curves. C. Bonatto Minella reported a related phenomenon and the difference between DSC analyses and volumetric measurements was ascribed to dissimilar experimental conditions.[38]

XRD analyses were performed on samples treated under a series of controlled conditions in order to have a better understanding of mechanisms of de/rehydrogenation in the

Table 1 The DSC peak temperatures of the $3NaBH_4/ScF_3$ at different heating rates under 0.1 MPa argon atmosphere

Sample	Heating rate/°C min^{-1}	Temperature of peaks/°C	
$3NaBH_4/ScF_3$	3	373	424
	5	383	440
	7	392	442
	10	397	452

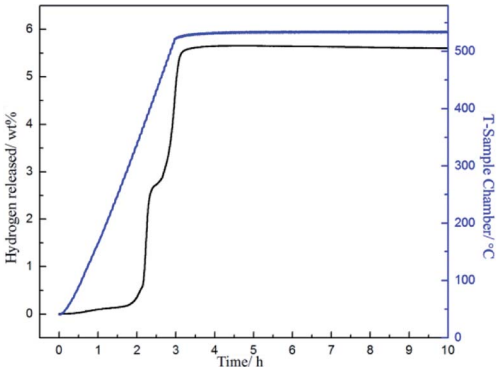

Fig. 2 TPD profile of the $3NaBH_4/ScF_3$ sample at a heating rate of 3 °C min^{-1}.

$3NaBH_4/ScF_3$ composite, as shown in Fig. 3. The results show that no new product can be found in the sample after ball milling, except $NaBH_4$ (JCPDS no. 09-0386) and ScF_3 (JCPDS no. 46-1243), which means that only physical mixing takes place during milling process. Before dehydrogenation at various temperatures of 300 °C, 420 °C and 530 °C, the loaded sample container was first placed under a 4.5 MPa H_2 pressure, then followed by a quick temperature rising and heat preservation. At last, the sample chamber was evacuated and powders were treated at the expected temperature for 3 h. After dehydrogenation at 300 °C under vacuum, it can be clearly seen in Fig. 4 that diffraction peaks from $NaBH_4$ in the $3NaBH_4/ScF_3$ composite shifted slightly from high angle side to lower angle side, demonstrating a lattice expansion of $NaBH_4$ after the first dehydrogenation.

On the basis of the XRD patterns and using the RIR analysis, the lattice parameters of $NaBH_4$ in ball milled sample is calculated to be: $a = 0.6165$ nm, $b = 0.6184$ nm, $c = 0.6153$ nm and $\alpha = \beta = \gamma = 90°$. After the first step dehydrogenation at 300 °C, the lattice constants of $NaBH_4$ changed into $a = 0.6185$ nm, $b = 0.6225$ nm, $c = 0.6166$ nm and $\alpha = \beta = \gamma = 90°$. Such a lattice expansion of $NaBH_4$ might be attributed to the fact that H^- was partially substituted by F^- in the unit cell. Similar phenomenon was also observed in some previous

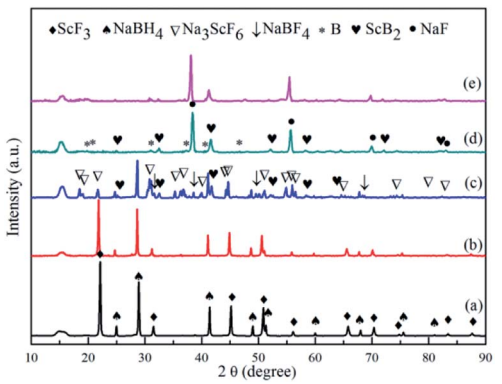

Fig. 3 XRD patterns of the $3NaBH_4/ScF_3$ composite after ball milling (a), dehydrogenated at 300 °C (b), dehydrogenated at 420 °C (c), fully dehydrogenated at 530 °C (d) and rehydrogenated at 420 °C (e).

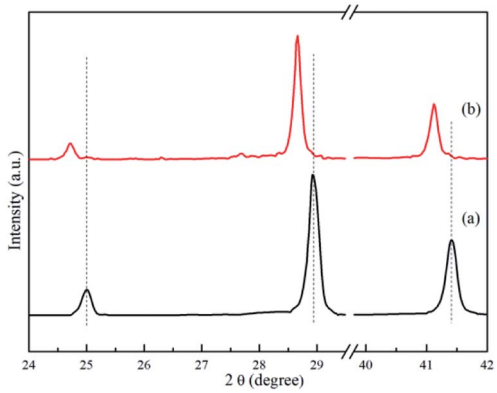

Fig. 4 XRD patterns of $3NaBH_4/ScF_3$ composite after ball milling (a) and after dehydrogenation at 300 °C (b) in the range of low diffraction angle.

works,[29,39–43] for which the lattice expansion was attributed to the formation of an intermediate compound $NaBH_xF_{4-x}$. In the present work, the formation of $NaBH_xF_{4-x}$ occurred at the first desorption step between $NaBH_4$ and ScF_3, together with releasing small amount of hydrogen, as also seen in the $3NaBH_4/NdF_3$, $3NaBH_4/PrF_3$, $3NaBH_4/HoF_3$ systems,[19,35,36] and was regarded as an energy favorable process in theory.[44] Upon heating at temperatures higher than 310 °C, along with the reduction of $NaBH_4$ and disappearance of ScF_3 (Fig. 3c), Na_3ScF_6 appeared in the system, indicating that a major reaction between $NaBH_4$ and ScF_3 occurred. It has been also indicated by Radovan Cerny *et al.* that in the case of $NaBH_4/ScCl_3$ system, Na_3ScCl_6 and $NaSc(BH_4)_4$ formed as a result of the reaction between $NaBH_4$ and $ScCl_3$.[32] Chong *et al.* reported that the reaction occurred at 250 °C between $NaBH_4$ and HoF_3 could produce $NaHo(BH_4)_4$ and $NaHo_2F_7$ phases.[36] In the $3NaBH_4/ScF_3$ composite, $NaSc(BH_4)_4$ might form upon heating and then decomposed to ScB_2 and H_2. Based on the XRD analysis, the second dehydrogenation step before 420 °C can be described as:

$$27NaBH_4 + 20ScF_3 = 8Na_3ScF_6 + 12ScB_2 + 54H_2 + 3NaBF_4 \quad (5)$$

Such a reaction has a theoretical hydrogen release of 2.53 wt%, close to the value measured from TPD for the second step dehydrogenation. At around 500 °C, the remaining $NaBH_4$ reacts with Na_3ScF_6 and $NaBF_4$ to produce NaF, ScB_2 and B, as shown in the indexed XRD pattern of Fig. 3d. Thus, the third dehydrogenation step can be described as follows:

$$33NaBH_4 + 8Na_3ScF_6 + 3NaBF_4 = 60NaF + 8ScB_2 + 66H_2 + 20B \quad (6)$$

with a theoretical hydrogen desorption value of 3.08 wt%. This value is also close to what is observed in the TPD analysis for the third dehydrogenation step. According to Garroni *et al.*,[45] $Na_2[B_{12}H_{12}]$ is usually a byproduct during desorption of $NaBH_4$ based composites, which forms in an intermediate step and is still present at the end of reaction. $Na_2[B_{12}H_{12}]$ is found to be a stable byproduct and cannot be re-hydrogenated to $NaBH_4$, thus is regarded as an unfavorable product for the reversibility.[46,47] However, the $Na_2[B_{12}H_{12}]$ phase was not found in the XRD pattern of the partial or the complete dehydrogenated $3NaBH_4/ScF_3$ samples, which means that very small amount or even no such a byproduct was generated during the decomposition of the $3NaBH_4/ScF_3$ composite.

3.2 Rehydrogenation in the $3NaBH_4/ScF_3$ composite

Fig. 3e shows the XRD pattern of the complete dehydrogenated $3NaBH_4/ScF_3$ composite (530 °C for 3 h) that is maintained under a pressure of 3.2 MPa H_2 at 420 °C for 10 h. The pattern shows no change compared to that of the complete dehydrogenated composite, which means that the latter one has no hydrogen absorption ability.

As the complete dehydrogenated $3NaBH_4/ScF_3$ composite shows no reversibility, the hydrogen absorption after the second dehydrogenation step was attempted to study the possible reversibility. The profiles of hydrogen absorption are given in Fig. 5a, which are obtained under the condition of 380 °C, 400 °C and 420 °C at 3.2 MPa H_2 pressure for the sample that has gone through dehydrogenation at 420 °C for 3 h. These curves clearly show the reversible hydrogen absorption of the partial dehydrogenated $3NaBH_4/ScF_3$ composite: under the pressure of 3.2 MPa H_2, a hydrogenation capacity of 1.59 wt% can be achieved at 420 °C for 8 h, while it can absorb 1.28 wt% at 400 °C and 1.19 wt% at 380 °C, respectively. By contrast, under 3.5 MPa hydrogen pressure, pure $NaBH_4$ shows no hydrogen absorption at 400 °C.[36]

The hydrogenation activation energy (E_{ab}) is generally utilized to discriminate kinetics of absorption, by analyzing the entire energy barriers of hydrogen absorption process. Based on the Johanson–Mehl–Avrami (JMA) model, the following equation can be used to evaluate absorption kinetics:[48]

$$\ln[-\ln(1 - \alpha_A)] = \eta \ln k + \eta \ln t \quad (7)$$

where $\alpha(t)$ is a function of time t, k is a parameter describing kinetic, η is the Avrami exponent which matches transformation mechanism. Then, the following Arrhenius equation is used to calculate E_{ab}:

$$k = A \exp\left(-\frac{E_{ab}}{RT}\right) \quad (8)$$

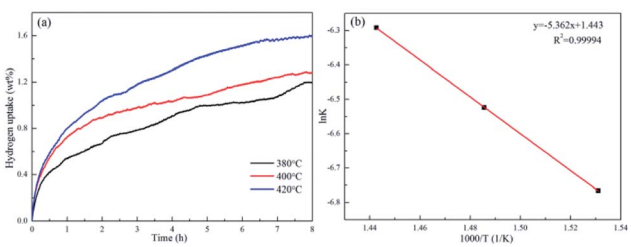

Fig. 5 Isothermal hydrogen absorption curves for the partially dehydrogenated $3NaBH_4/ScF_3$ composite sample at temperatures of 380 °C, 400 °C and 420 °C (a) and the ln k-1000/T fitting plot (b).

where A represents temperature-independent constant, R represents universal gas constant, and T represents the absolute temperature. The scheme of ln k *versus* 1000/T, which is shown in Fig. 5, displays a good linear relationship. Therefore, the E_{ab} value obtained from the slope is therefore estimated to be 44.58 kJ mol^{-1} H_2 for the partially dehydrogenated $3NaBH_4/ScF_3$ composite.

To elucidate the mechanism of hydrogen absorption in the partially dehydrogenated $3NaBH_4/ScF_3$ composite, XRD analysis is carried out on the rehydrogenated sample and the result is shown in Fig. 6. The $3NaBH_4/ScF_3$ sample was dehydrided at 420 °C for 3 h in vacuum and then rehydrogenated at 420 °C for 10 h under the pressure of 3.2 MPa H_2. In Fig. 6, the diffraction peaks from $NaBF_4$ and ScB_2 phases became weaker and even disappeared along with the increment in peak intensities of $NaBH_4$ and ScF_3 as compared to those in Fig. 3c. Therefore, the hydrogen absorption in the partial dehydrogenated $3NaBH_4/ScF_3$ composite follows exactly the reverse reaction path of the second step dehydrogenation. That is, the rehydrogenation consumes Na_3ScF_6, $NaBF_4$ and ScB_2, accompanied with the regeneration of $NaBH_4$ and ScF_3. Compared to the completely dehydrogenated $3NaBH_4/ScF_3$ composite, the partially dehydrogenated composite contains Na_3ScF_6 and $NaBF_4$ phases, indicating that these two phases play the key role for the rehydrogenation.

The results of FTIR analyses for the ball-milled $3NaBH_4/ScF_3$ sample, sample dehydrogenated at 420 °C for 3 h and corresponding products rehydrogenated at 400 °C for 3 h can be found in Fig. 7. In Fig. 7a, the FTIR spectrum of sample after ball milling has the signatures of B–H stretching band in the position of 2226 cm^{-1}, 2306 cm^{-1} and 2366 cm^{-1}, and B–Hbending band peak at 1119 cm^{-1}, all of which are supposed to be originated from borohydride. These peaks are considered to be from $NaBH_4$.[19] However, it should be noted that, the height of those peaks, which represent the intensity of B–H bonds vibration from the $[BH_4]^-$ group, gradually become weaker as dehydrogenation reaction proceeds, indicating the decomposition of $NaBH_4$, as seen at 1121 cm^{-1}, 2221 cm^{-1}, 2338 cm^{-1} and 2369 cm^{-1} in Fig. 7b. According to the work of D. Syamala,[44] peak located at 1065 cm^{-1} can be marked as $[BF_4]^-$asymmetric stretching, indicating the formation of $NaBF_4$ after the second step dehydrogenation, which is in good agreement with the XRD results (Fig. 3c). In Fig. 7c, the signatures of $[BH_4]^-$ bending at 1120 cm^{-1} and $[BH_4]^-$ stretching at 2223 cm^{-1}, 2304 cm^{-1} and 2359 cm^{-1} were clearly revealed for the rehydrogenated sample and the intensity of these peaks increased, indicating the regeneration of $NaBH_4$.[49] Meantime, the peak from $[BF_4]^-$ asymmetric stretching disappeared after rehydrogenation, showing the consumption of $NaBF_4$ along with rehydrogenation. Peaks at wave numbers between 1330 cm^{-1} and 1800 cm^{-1} (Fig. 7a) were subtracted from the unavoidable moisture absorption and atmospheric humidity absorbed by the sample during measurement, while peak located at around 3745 cm^{-1} was identified as stretching band vibration of O–H.[50]

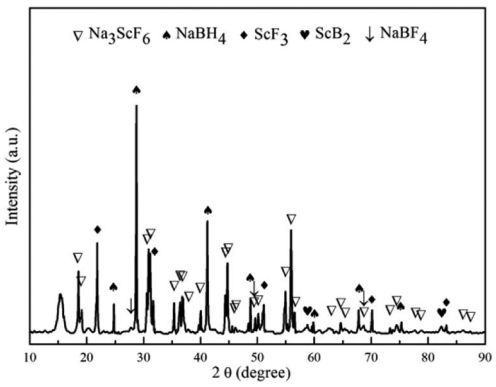

Fig. 6 XRD pattern of the partially dehydrogenated $3NaBH_4/ScF_3$ composite sample after rehydrogenation.

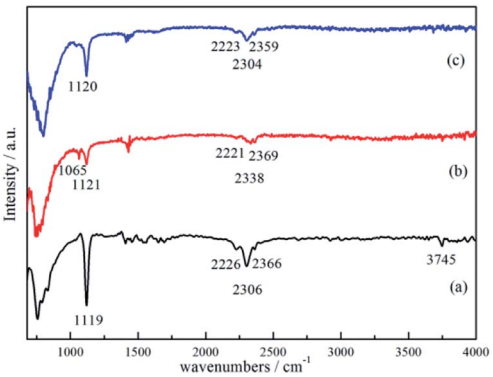

Fig. 7 FTIR spectra of the $3NaBH_4/ScF_3$ composite after ball-milling (a), half dehydrogenated $3NaBH_4/ScF_3$ sample (b), rehydrogenation of partially dehydrogenated $3NaBH_4/ScF_3$ sample (c).

3.3 Mechanisms of hydrogenation in $3NaBH_4/ScF_3$ composite

It is shown in the present work that the hydrogen storage performance of $NaBH_4$ can be effectively improved by introducing ScF_3 as a reagent. In particular, rehydrogenation can be achieved in the partially dehydrogenated $3NaBH_4/ScF_3$ composite. Analyses revealed that both Sc^{3+} cation and F^- anion show irreplaceable importance during the re/dehydrogenation processes of the composite. Firstly, F anion can replace H anion in the initial process of dehydrogenation, from $NaBH_4$ to form $NaBH_xF_{4-x}$. Then, Sc cation loses electron to form ScB_2, in which Sc cation has the calculated valence of +4.08,[51] rather than served as a three-valent cation. This is accompanied with the formation of hydrogen gas. Meanwhile, during the second dehydrogenation step, a portion of F anions from ScF_3 incorporate into Na_3ScF_6 crystallites, which might serve as the nucleation center for the growth of other products.

It has been established that the regeneration of $NaBH_4$ in the $NaBH_4$–MF_x systems is associated with electronegativity (χ_p) of the metal cations.[52] Previous works have shown that after adding transition metal fluorides into $NaBH_4$ based composites, when the Pauling's electronegativity of the transition metal lies in around between 1.23–1.54, hydrogen sorption reversibility has larger thermodynamic tendency to occur.[52] The χ_p value of Sc^{3+} is 1.415, which lies in such specific range, thus the

regeneration of $NaBH_4$ in the dehydrided $3NaBH_4/ScF_3$ system is favorable.[53]

Using a database of density functional theory,[54–56] the enthalpies of desorption reactions are calculated to be 41.01 kJ mol^{-1} H_2 for the second dehydriding step, and 43.31 kJ mol^{-1} H_2 for the final step. These values are comparably higher than the values obtained from DSC/TG analyses, but significant lower than that of pristine $NaBH_4$ (108 ± 3 kJ mol^{-1} of H_2).[57] The differences between the calculated and measured enthalpies can be explained by fact that H^- was partially substituted by F^- in $NaBH_4$, which is also observed in other $NaBH_4$ based systems containing fluorides.[58] However, the enthalpy for complete dehydrogenation is still fairly high, about 56.97 kJ mol^{-1} H_2 calculated from DSC analyses. Consequently, the rehydrogenation of the complete dehydrided $3NaBH_4/ScF_3$ composite is difficult from the thermodynamic point of view.[52]

During the rehydrogenation process, the experimental results show that only partial dehydrogenated products ($NaBF_4$ + ScB_2 + Na_3ScF_6) have reversibility, while the final dehydriding products (NaF + ScB_2 + B) cannot be rehydrogenated. Apart from the thermodynamic factors, this might also be understood from structural similarity between $[BF_4]^-$ in $NaBF_4$ and $[BH_4]^-$ in $NaBH_4$, which may facilitate the regeneration of $NaBH_4$ through the exchange between H^- and F^-. The structural similarity was also observed between dehydrogenated and rehydrogenated products in the $3NaBH_4/LnF_3$ systems, which led to the improved rehydrogenation kinetics in these systems.[25] Researchers have also found that substitution reaction could be well understood from the hydride–fluoride isostructure, which has been proposed and confirmed in various hydrides–fluorides compounds having different stoichiometries.[59–61]

4 Conclusions

In this study, the $3NaBH_4/ScF_3$ composite was prepared through mechanical milling. The behaviors and mechanisms of hydrogen de/absorption of the composite were explained by using TPD, DSC/TG, XRD and FTIR techniques. Following are the summarized results:

(1) TPD and DSC analyses confirmed that $NaBH_xF_{4-x}$ compound formed at the early dehydriding stage due to the partial substitution of H^- anion by F^- anion in $NaBH_4$, releasing about 0.19 wt% of hydrogen. When temperature further increases, Na_3ScF_6, $NaBF_4$ and ScB_2 formed through the reaction between $NaBH_4$ and ScF_3 with 2.52 wt% of hydrogen released. Finally, the reaction of residual $NaBH_4$ with Na_3ScF_6 produces NaF, B and ScB_2, releasing about 2.83 wt% of hydrogen.

(2) The partially dehydrogenated products, Na_3ScF_6, ScB_2 and $NaBF_4$, can be rehydrogenated to generate $NaBH_4$ with an activation energy of 44.58 kJ mol^{-1} H_2. In contrast, the fully dehydrogenated products, NaF + ScB_2 + B, cannot be hydrogenated. The hydrogen sorption reversibility of the partially dehydrogenated composite can be understood through thermodynamic point of view and the structural similarity between $[BF_4]^-$ in $NaBF_4$ and $[BH_4]^-$ in $NaBH_4$.

Conflicts of interest

There are no conflicts to declare.

Acknowledgements

This work was supported by National Nature Science Foundation (No. 51771112), the Shanghai Science and Technology Commission under No. 14JC1491600 and Shanghai Education Commission "Shuguang" scholar project (16SG08).

Notes and references

1 W. Li, X. F. Gao, X. G. Wang, D. H. Xiong, P. P. Huang, W. G. Song, X. Q. Bao and L. F. Liu, *J. Power Sources*, 2016, **330**, 156.
2 T. da Silva Veras, T. S. Mozer and A. da Silva César, *Int. J. Hydrogen Energy*, 2017, **42**, 2018.
3 Q. W. Lai, M. Paskevicius, D. A. Sheppard, C. E. Buckley, A. W. Thornton, M. R. Hill, Q. F. Gu, J. F. Mao, Z. G. Huang, H. K. Liu, Z. P. Guo, A. Banerjee, S. Chakraborty, R. Ahuja and K.-F. Aguey-Zinsou, *ChemSusChem*, 2015, **8**, 2789.
4 L. Schlapbach and A. Züttel, *Nature*, 2001, **414**, 353.
5 J. F. Mao and D. H. Gregory, *Energies*, 2015, **8**, 430.
6 W. Li, X. F. Gao, D. H. Xiong, F. Xia, J. Liu, W. G. Song, J. Y. Xu, S. M. Thalluri, M. F. Cerqueira, X. L. Fu and L. F. Liu, *Chem. Sci.*, 2017, **8**, 2952.
7 F. Z. Song, W. Li, G. Q. Han and Y. J. Sun, *ACS Appl. Energy Mater.*, 2018, **1**, 3.
8 W. Li, D. H. Xiong, X. F. Gao, W. G. Song, F. Xia and L. F. Liu, *Catal. Today*, 2017, **287**, 122.
9 W. Li, X. G. Wang, D. H. Xiong and L. F. Liu, *Int. J. Hydrogen Energy*, 2016, **41**, 9344.
10 P. P. Silva, R. A. Ferreira, F. B. Noronha and C. E. Hori, *Catal. Today*, 2017, **289**, 211.
11 W. Li, X. Gao, D. Xiong, F. Wei, W. G. Song, J. Xu and L. Liu, *Adv. Energy Mater.*, 2017, **7**, 1602579.
12 C. Y. Cao, C. Q. Chen, W. Li, W. G. Song and W. Cai, *ChemSusChem*, 2010, **3**, 1241.
13 J. F. Mao, Q. F. Gu, Z. P. Guo and H. K. Liu, *J. Mater. Chem. A*, 2015, **3**, 11269.
14 S. Orimo, Y. Nakamori, J. R. Eliseo, A. Züttel and C. M. Jensen, *Chem. Rev.*, 2007, **107**, 4111.
15 P. Chen and M. Zhu, *Mater. Today*, 2008, **11**, 36.
16 D. M. F. Santos and C. A. C. Sequeira, *Renewable Sustainable Energy Rev.*, 2011, **15**, 3980.
17 Y. F. Liu, Y. X. Yang, M. X. Gao and H. G. Pan, *Chem. Rec.*, 2016, **16**, 189.
18 U. B. Demirci, O. Akdim, J. Andrieux, J. Hannauer, R. Chamoun and P. Miele, *Fuel Cells*, 2010, **10**, 335.
19 L. N. Chong, J. X. Zou, X. Q. Zeng and W. J. Ding, *J. Mater. Chem. A*, 2013, **1**, 3983.
20 M. Yadav and Q. Xu, *Energy Environ. Sci.*, 2012, **5**, 9698.
21 G. Moussa, R. Moury, U. B. Demirci, T. Sener and P. Miele, *Int. J. Energy Res.*, 2013, **37**, 825.

22 J. Urgnani, F. J. Torres, M. Palumbo and M. Baricco, *Int. J. Hydrogen Energy*, 2008, **33**, 3111.
23 T. J. Frankcombe, *Chem. Rev.*, 2011, **112**, 2164.
24 P. E. de Jongh and P. Adelhelm, *ChemSusChem*, 2010, **3**, 1332.
25 J. J. Vajo, T. T. Salguero, A. F. Gross, S. L. Skeith and G. L. Olson, *J. Alloys Compd.*, 2007, **446**, 409.
26 A. T. Dinsdale, *Calphad*, 1991, **15**, 317.
27 T. Czujiko, R. A. Varin, Z. Zaranski and Z. S. Wronski, *Arch. Metall. Mater.*, 2010, **55**, 539.
28 T. D. Humphries, G. N. Kalantzopoulos, I. Llamas-Jansa, J. E. Olsen and B. C. Hauback, *J. Phys. Chem. C*, 2013, **117**, 6060.
29 J. F. Mao, Z. P. Guo, I. P. Nevirkovets, H. K. Liu and S. X. Dou, *J. Phys. Chem. C*, 2012, **116**, 1596.
30 S. A. Jin, J. H. Shim, Y. W. Cho, K. W. Yi, O. Zabara and M. Fichtner, *Scr. Mater.*, 2008, **58**, 963.
31 J. X. Zou, L. J. Li and X. Q. Zeng, *Int. J. Hydrogen Energy*, 2012, **37**, 17118.
32 R. Cerny, G. Severa, D. B. Ravnsbæk, Y. Filinchuk, V. D'Anna, H. Hagemann, D. Haase, C. M. Jensen and T. R. Jensen, *J. Phys. Chem. C*, 2010, **114**, 1357.
33 D. B. Ravnsbæk, Y. Filinchuk, R. Cerny, M. B. Ley, D. Haase, H. J. Jakobsen, J. Skibsted and T. R. Jensen, *Inorg. Chem.*, 2010, **49**, 3801.
34 L. N. Chong, J. X. Zou, X. Q. Zeng and W. J. Ding, *J. Mater. Chem. A*, 2015, **3**, 4493.
35 L. N. Chong, J. X. Zou, X. Q. Zeng and W. J. Ding, *J. Mater. Chem. A*, 2013, **1**, 13510.
36 L. N. Chong, J. X. Zou, X. Q. Zeng and W. J. Ding, *Int. J. Hydrogen Energy*, 2014, **39**, 14275.
37 H. E. Kissinger, *Anal. Chem.*, 1957, **29**, 1702.
38 C. Bonatto Minella, S. Garroni, C. Pistidda, R. Gosalawit-Utke, G. Barkhordarian, C. Rongeat, I. Lindemann, O. Gutfleisch, T. R. Jensen, Y. Cerenius, J. Christensen, M. D. Baró, R. Bormann, T. Klassen and M. Dornheim, *J. Phys. Chem. C*, 2011, **115**, 2497.
39 L. C. Yin, P. Wang, X. D. Kang, C. H. Sun and H. M. Cheng, *Phys. Chem. Chem. Phys.*, 2007, **9**, 1499.
40 R. Gosalawit-Utke, J. M. Bellosta von Colbe, M. Dornheim, T. R. Jensen, Y. Cerenius, C. Bonatto Minella, M. Peschke and R. Bormann, *J. Phys. Chem. C*, 2010, **114**, 10291.
41 H. W. Brinks, A. Fossdal and B. C. Hauback, *J. Phys. Chem. C*, 2008, **112**, 5658.
42 Y. F. Liu, F. H. Wang, Y. H. Cao, M. X. Gao, H. G. Pan and Q. D. Wang, *Energy Environ. Sci.*, 2010, **3**, 645.
43 Z. Z. Fang, X. D. Kang, Z. X. Yang, G. S. Walker and P. Wang, *J. Phys. Chem. C*, 2011, **115**, 11839.
44 D. Syamala, V. Rajendran, R. K. Natarajan and S. Moorthy Badu, *Cryst. Growth Des*, 2007, **7**, 1695.
45 S. Garroni, C. Milanese, D. Pottmaier, G. Mulas, P. Nolis, A. Girella, R. Caputo, D. Olid, F. Teixdor, M. Baricco, A. Marini, S. Suriñach and M. D. Baró, *J. Phys. Chem. C*, 2011, **115**, 16664.
46 J. H. Her, W. Zhou, V. Stavila, C. M. Brown and T. J. Udovic, *J. Phys. Chem. C*, 2009, **113**, 11187.
47 R. Caputo, S. Garroni, D. Olid, F. Teixidor, S. Surinach and M. D. Baro, *Phys. Chem. Chem. Phys.*, 2010, **12**, 15093.
48 P. S. Rudman, *J. Less-Common Met.*, 1983, **89**, 93.
49 T. Sato, K. Miwa, Y. Nakamori, K. Ohoyama, H. W. Li, T. Noritake, M. Aoki, S. I. Towata and S. I. Orimo, *Phys. Rev. B*, 2008, **77**, 104114.
50 A. M. Olsson and L. Salmén, *Carbohydr. Res.*, 2004, **339**, 813.
51 R. S. Roth and S. Schneider, National Bureau of Standards, 1972, p. 364.
52 Y. Nakamori, K. Miwa, A. Ninomiya, H. W. Li, N. Ohba, S. I. Towata, A. Züttel and S. I. Orimo, *Phys. Rev. B*, 2006, **74**, 045126.
53 K. Y. Li and D. F. Xue, *J. Phys. Chem. A*, 2006, **110**, 11332.
54 A. Jain, G. Hautier, S. P. Ong, C. J. Moore, C. C. Fischer, K. A. Persson and G. Ceder, *Phys. Rev. B: Condens. Matter Mater. Phys.*, 2011, **84**, 045115.
55 A. Jain, S. P. Ong, G. Hautier, W. Chen, W. D. Richards, S. Dacek, S. Cholia, D. Gunter, D. Skinner, G. Ceder and K. A. Persson, *APL Mater.*, 2013, **1**, 011002.
56 L. C. Yin, P. Wang, Z. Z. Fang and H. M. Cheng, *Chem. Phys. Lett.*, 2008, **450**, 318.
57 P. Martelli, R. Caputo, A. Remhof, P. Mauron, A. Borgschulte and A. Züttel, *J. Phys. Chem. C*, 2010, **114**, 7173.
58 L. N. Chong, J. X. Zou, X. Q. Zeng and W. J. Ding, *J. Mater. Chem. A*, 2014, **2**, 8557.
59 A. Bouamrane, J. P. Laval, J.-P. Soulie and J. P. Bastide, *Mater. Res. Bull.*, 2000, **35**, 545.
60 J. P. Soulié, J. P. Laval and A. Bouamrane, *Solid State Sci.*, 2003, **5**, 273.
61 Q. Zhou and B. J. Kennedy, *J. Solid State Chem.*, 2004, **177**, 654.